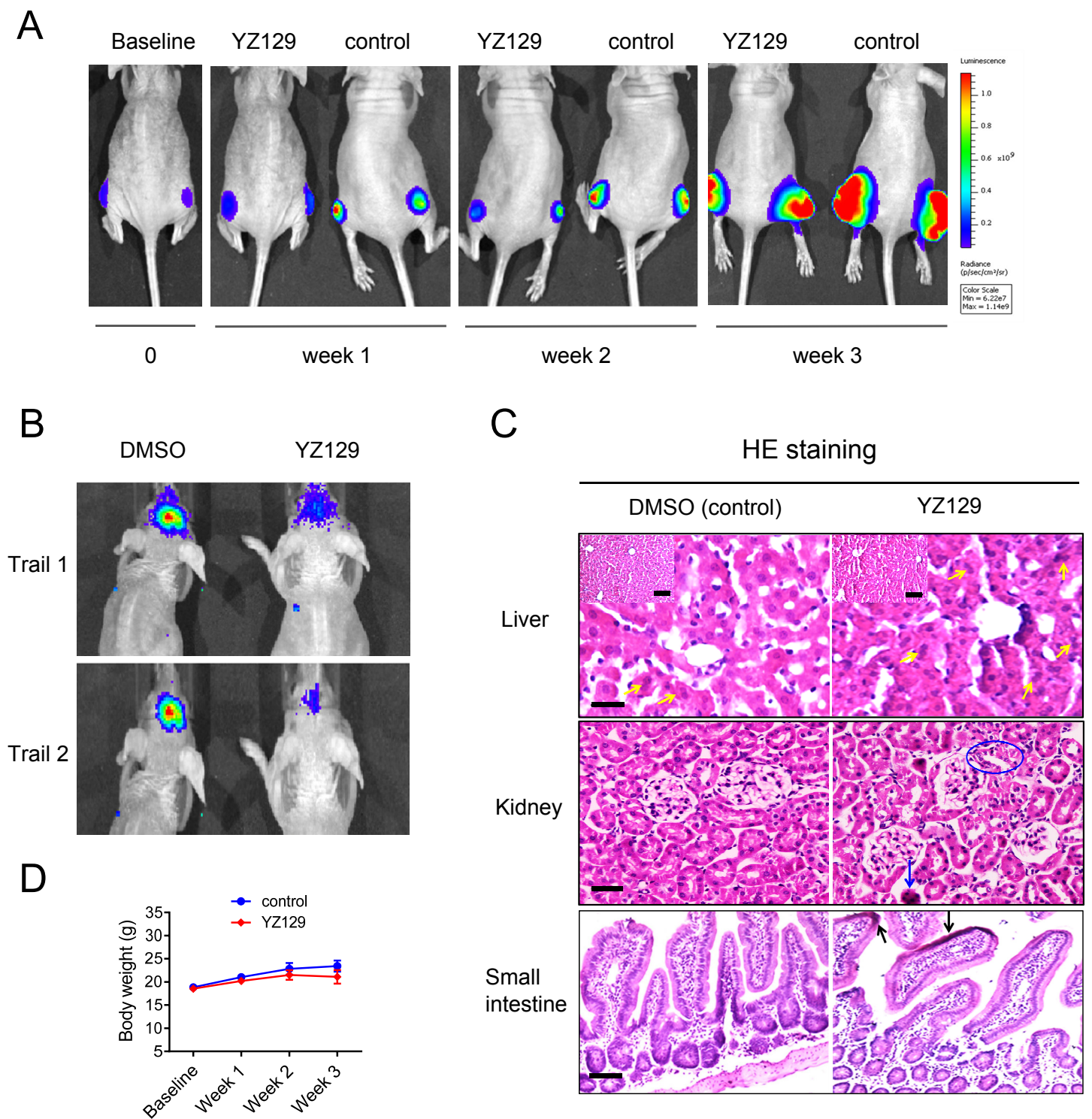


**Figure S1 |The impact of YZ129 on GBM cell apoptosis. (Related to Figures 2 and 6)**

- (A) Representative immunostaining images showing Ki67 (red) and cleaved-caspase3 (green) expression in U87 cells treated with DMSO or YZ129 (5  $\mu$ M) for 24 h. Scale bar, 50  $\mu$ m. The nuclei were stained with DAPI (blue). Percentage of Ki67 positive cells or the relative intensities of caspase 3 staining were plotted on the right (mean  $\pm$  S.D., n=5).
- (B) Heatmap showing the differential expression levels of apoptosis-associated proteins in U87 cells treated with DMSO or YZ129. Red, upregulation; blue, downregulation.



**Figure S2 | YZ129 suppressed U87 cell growth *in vivo* and assessment of YZ129 toxicity. (Related to Figure 3)**

(A) Representative bilateral bioluminescence images of nude mice bearing U87-Luc xenograft tumors. Mice were either vehicle-treated or YZ129-treated.

(B) Two sets of representative bioluminescence images of U87-Luc orthotopic xenograft tumors from nude mice treated with vehicle or YZ129.

(C) Representative HE staining results of healthy tissues derived from liver (Top panel; yellow arrow, binuclear hepatocytes), kidney (Middle panel; blue ring, thinner tubular wall; blue arrow, cells with pyknosis in the nuclei) and small intestine (Bottom panel; black arrow, cells with nuclear pyknosis) in mice treated with vehicle (DMSO as control) or YZ129. No major toxic damages to tissues were noted. Scale bar 20  $\mu$ M.

(D) Body weight measured in mice with U87 xenografts from week 0 to week 3 (mean  $\pm$  SD, n=4).

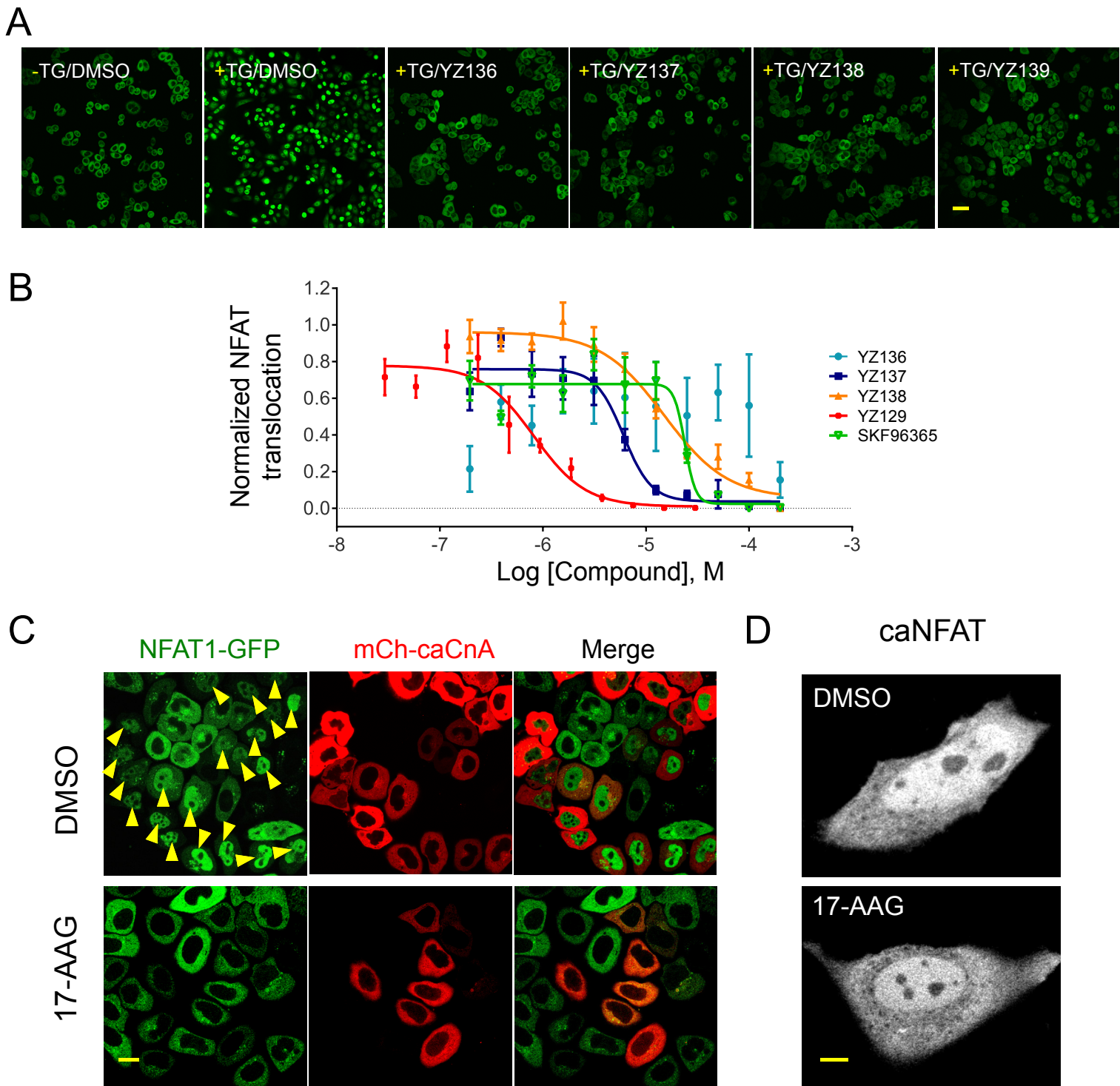
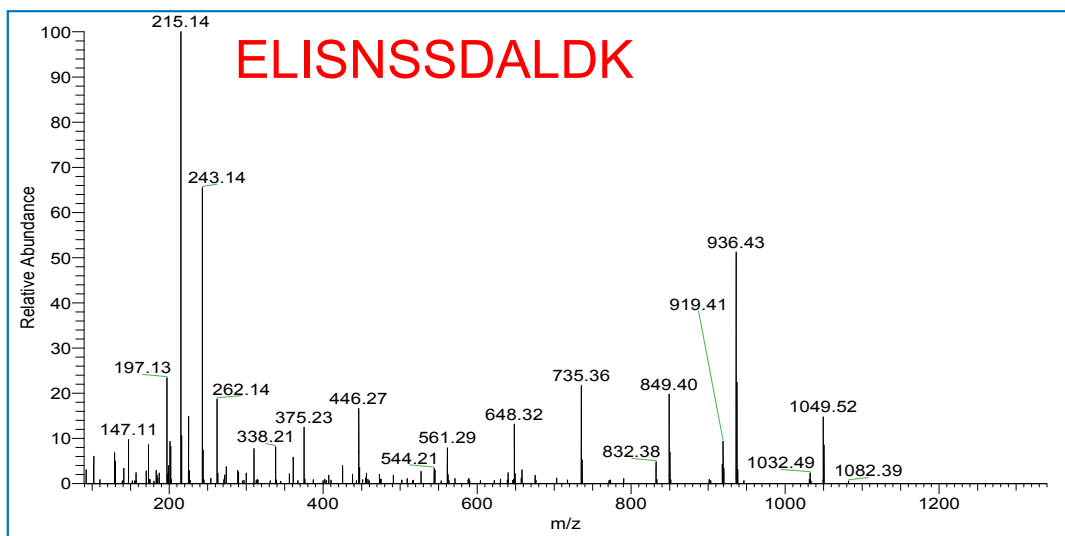
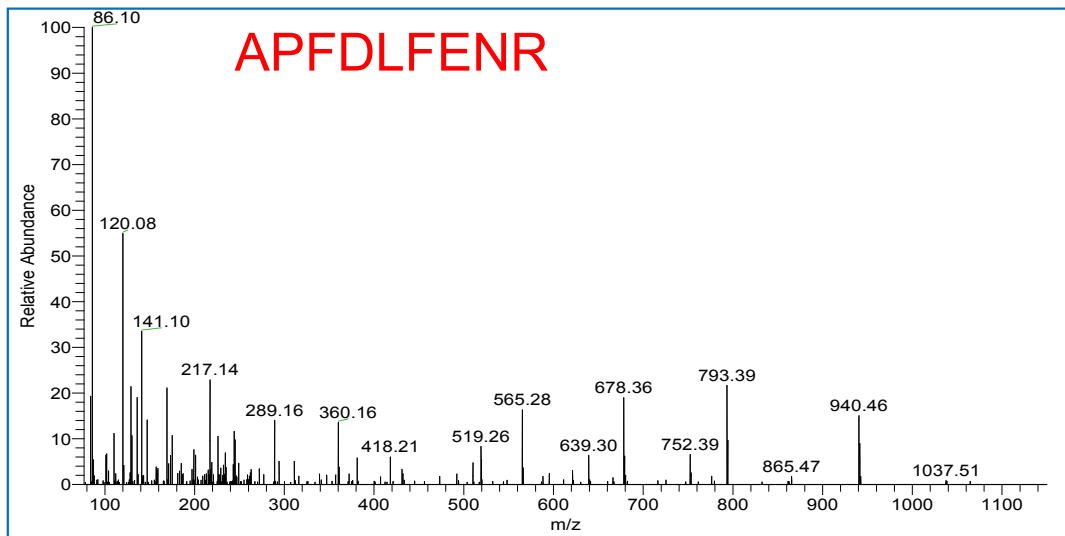


**Figure S3 | The NFAT-inhibitory activity of the azide analogues of YZ129 (YZ136-139, A-B) and 17-AAG (C-D). (Related to Figure 5)**

- (A) Representative confocal images showing the inhibitory effect of YZ136-139 on NFAT nuclear translocation. DMSO was used as control. TG was added to elicit calcium store depletion and NFAT nuclear entry. Scale bar, 40  $\mu\text{m}$ .
- (B) The inhibitory activity curves of YZ129 azide analogues (NFAT nuclear translocation as readout). YZ137 stood out as the best among the three analogues with an  $\text{IC}_{50}$  value of  $7.7 \pm 2.4 \mu\text{M}$  (mean  $\pm$  s.e.m.,  $n = 4$ ).
- (C) The effect of 17-AAG (50  $\mu\text{M}$ ) on constitutively activated calcineurin (caCnA)-induced NFAT nuclear translocation. Calcineurin was tagged with mCherry (mCh) and transfected into an NFAT1-GFP stable cell line. caCnA-mediated NFAT nuclear translocation was inhibited by 17-AAG. Scale bar, 20  $\mu\text{m}$ .
- (D) The effect of 17-AAG (50  $\mu\text{M}$ ) on constitutively active NFAT1 (caNFAT1), in which caNFAT1 was labeled with GFP and transfected into HeLa cells. 17-AAG had no effect on the nuclear localization of caNFAT1. Scale bar, 10  $\mu\text{m}$ .

A



B

```

1 MPEETQTQDQ PMEEEEVETF AFQAEIAQLM SLIINTFYNS KEIFLREELIS NSSDALDKIR
61 YESLTDPSKL DSGKELHINL IPNKQDRTLT IVDTGIGMTK ADLNNLGTI AKSGTKAFME
121 ALQAGADISM IGQFGVGFYS AYLVAEKVTV ITKHNDDEQY AWESSAGGSF TVRTDTGEPM
181 GRGTKVILHL KEDQTEYLEE RRIKEIVKKH SQFIGYPITL FVEKERDKEV SDDEAE EKED
241 KEEEEKEEEK ESEDKPEIED VGSDEEEEEK DGDKKKKKKI KEKYIDQEEL NKT KPIWTRN
301 PDDITNEEYG EFYKSLTNDW EDHLAVKHFS VEGQLEFRAL LFPVRRAPFD LFENRKKKNN
361 IKLYVRRVFI MDNCEELIPE YLNFIRGVVD SEDLPLNISR EMLQQSKILK VIRKNLVKKC
421 LELFTELAED KENYKKFYEQ FSKNIKLG IH EDSQNRK KLS ELLRYTSAS GDEMVLKDY
481 CTRMKENQKH IYYITGETKD QVANSAFVER LRKHGLEVIY MIEPIDEYCV QQLKEFEGKT
541 LVSVTKEGLE LPEDEEEKKK QEEKKTKFEN LCKIMKDILE KKVEKVVSN RLVTSPCCIV
601 TSTYGW TANM ERIMKAQALR DNSTMGYMAA KKHLEINPDH SIIETLRQKA EADKNDKSVK
661 DLVILLYETA LLSSGF SLED PQTHANRIYR MIKLG LGIDE DDPTADDTSA AVTEEMPPLE
721 GDDDTSRMEE VD

```

**Figure S4 | Identification of HSP90 as a biotin-YZ137 binder by mass spectrometry (MS).**

**(Related to Figure 5)**

(A) Representative MS peaks corresponding to peptide fragments derived from HSP90.

(B) Peptide fingerprints identified by MS were mapped to the primary sequence of human HSP90 (red).

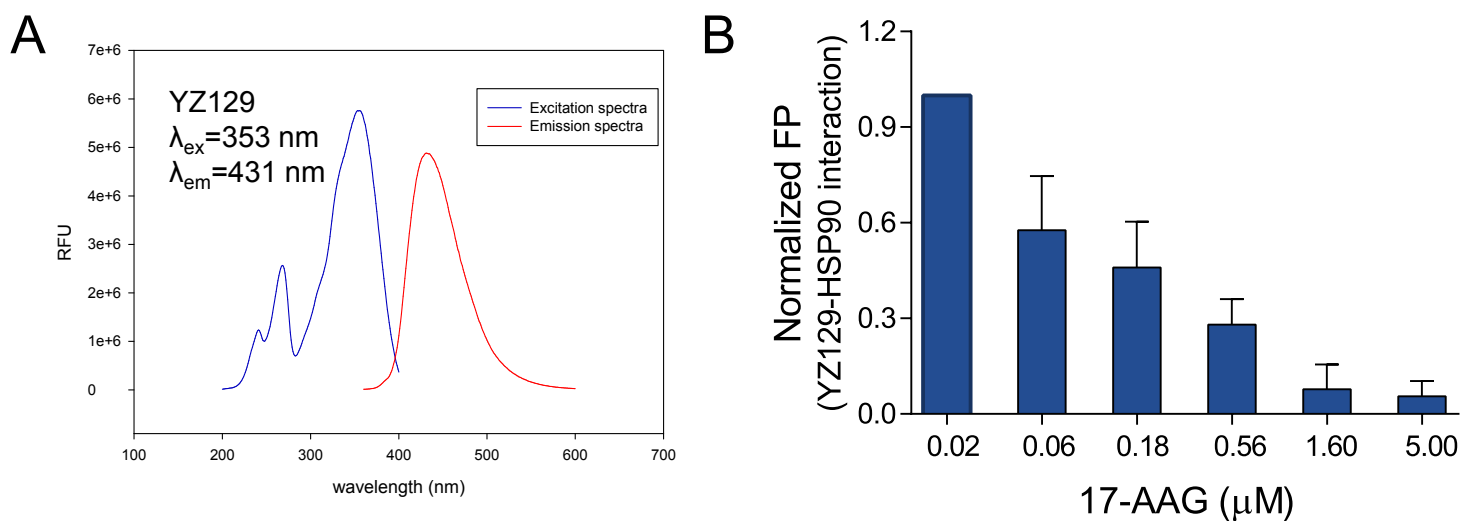


**Figure S5 | Fluorescence spectra of YZ129 and assessment of the reversibility of the YZ129-HSP90 interaction. (Related to Figure 5)**

(A) Representative excitation and emission spectra of YZ129.

(B) The competitive binding of 17-AAG to the HSP90-YZ129 complex revealed by the reduction of FP signals. The normalized fluorescence polarization at 460 nm (from YZ129) was plotted against increasing concentrations of 17-AAG. (mean  $\pm$  s.e.m., n= 3)

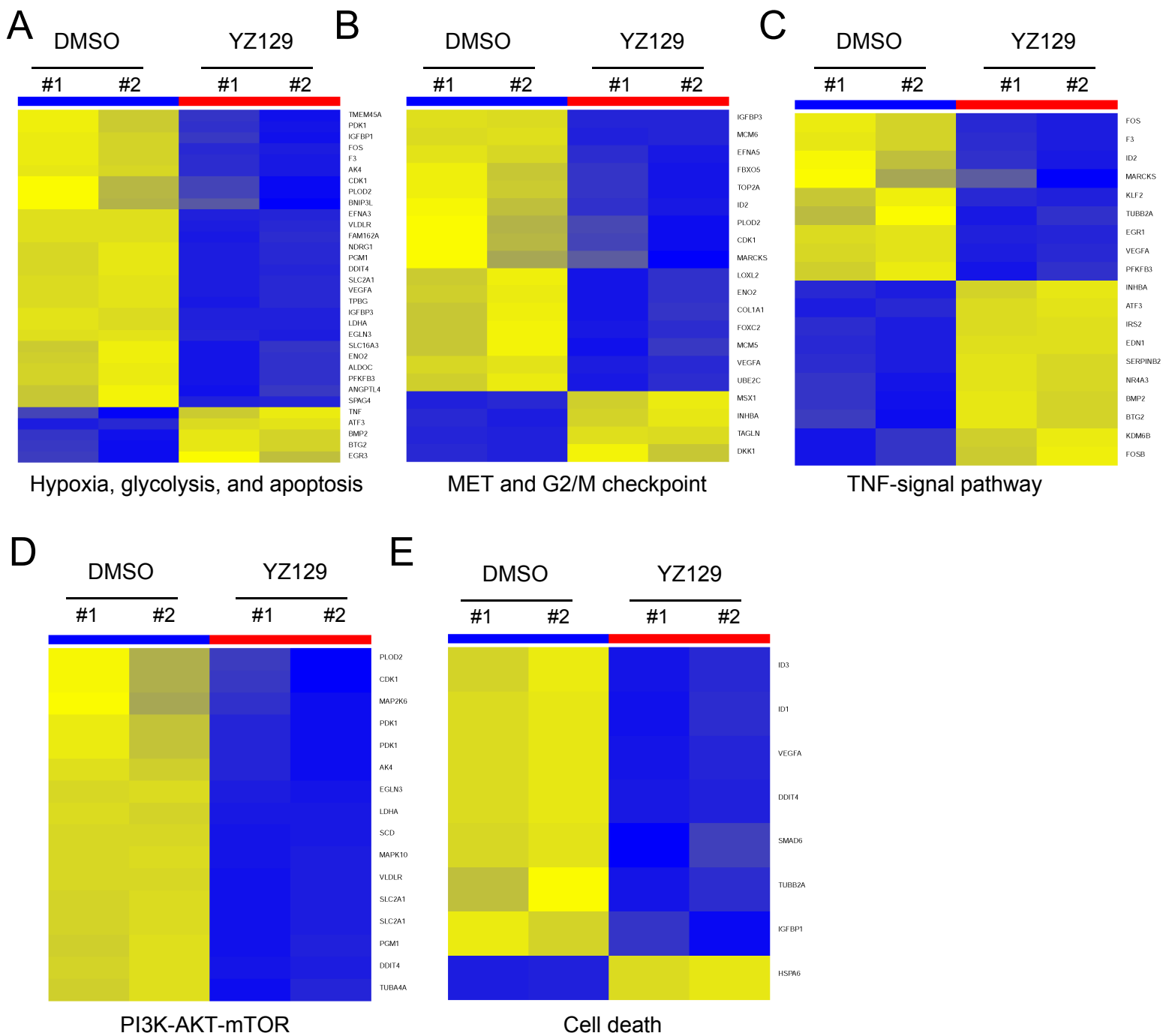


**Figure S6 | Heatmaps of differentially expressed genes (DEGs; DMSO vs YZ129-treated U87 GBM cells) classified according to their functions. (Related to Figure 6)**

(A) Heatmap of DEGs involved in hypoxia (downregulation), glycolysis (downregulation), and apoptosis (upregulation).

(B) Heatmap of DEGs involved in MET and the G2/M checkpoint (downregulation).

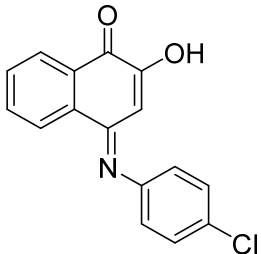
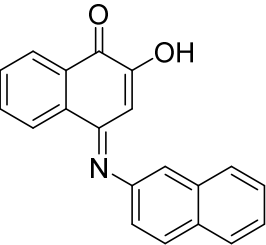
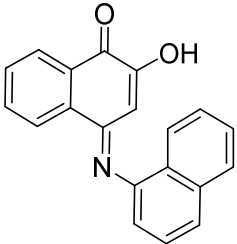
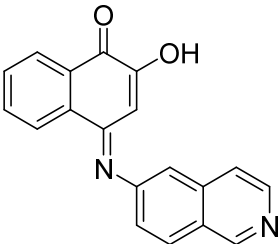
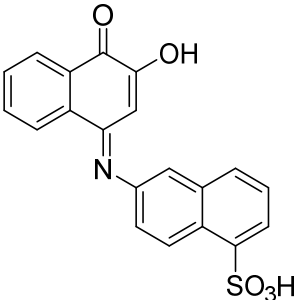
(C) Heatmap of DEGs involved in the TNF signaling pathway.

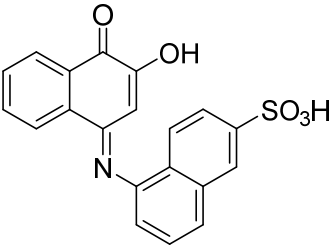
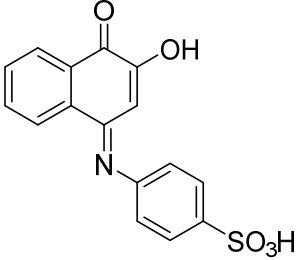
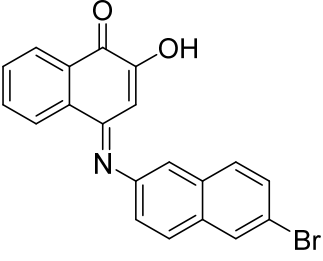
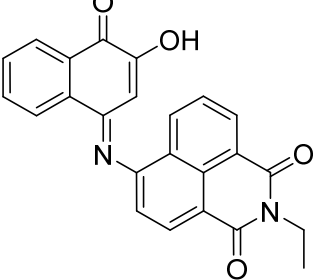
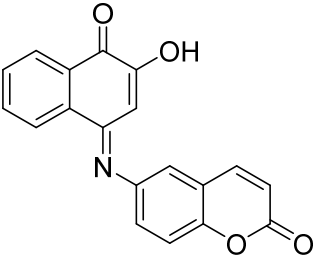
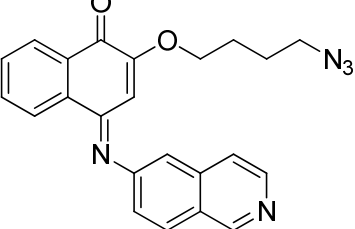
(D) Heatmap of DEGs involved in the PI3K-AKT-mTOR signaling pathway (downregulation).

(E) Heatmap of DEGs involved in cell death (downregulation) as well as the feedback upregulated gene HSPA6 (HSP70) following HSP90 inhibition.

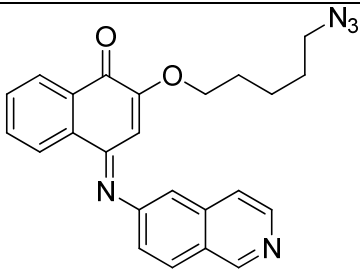
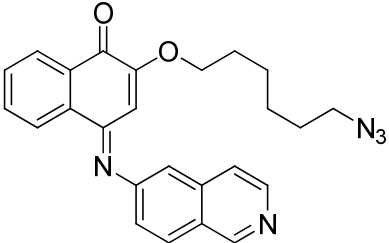
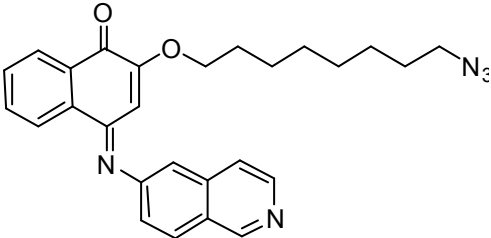
**Table S1.** The chemical structures of representative compounds used in the screening (YZ01-YZ52; **Figure 1A**) as well as their primary activities determined by the NFAT nuclear translocation assay (evaluated by the Z' score at 200  $\mu$ M for each compound). A Z' score of >1.5 or <-1.5 is deemed as significant. (**Related to Figure 1**). **Table S1** was shown in excel **Table S1** file.

**Table S2.** Structures of analogues of YZ01 (YZ126-YZ135) as well as azide derivatives of YZ129 (YZ136-YZ139). Their primary activities were determined by the NFAT nuclear translocation assay (Z' score value at 200  $\mu$ M of each compound). (**Related to Figure 1**)

Compound ID	Structure of the compounds	Z' score value	IC <sub>50</sub> value ( $\mu$ M)
YZ126		-1.31	3.6 $\pm$ 0.1
YZ127		1.29	NA
YZ128		-1.05	191.8 $\pm$ 12.9
YZ129		<b>-1.75</b>	<b>0.8 <math>\pm</math> 0.1</b>
YZ130		0.43	NA

YZ131		0.01	NA
YZ132		-0.87	NA
YZ133		1.25	NA
YZ134		-0.23	NA
YZ135		NA	9.3 ± 1.1
YZ136		NA	NA



YZ137		NA	7.7 ± 2.4
YZ138		NA	15.6 ± 0.7
YZ139		NA	NA

**Table S3.** Inhibitory activities of the compounds on NFAT nuclear translocation and HSP90.  
(Related to Figures 1 and 5)

Compounds	R	NFAT translocation	HSP90
		IC <sub>50</sub> /μM	IC <sub>50</sub> /nM
YZ-01		60.0	>1000
YZ126	4-Cl-Ph	3.6 ± 0.1	60.8
YZ127	naphthalen-2-yl	NA	NA
YZ128	naphthalen-1-yl	191.8 ± 12.9	NA
YZ129	isoquinolin-6-yl	0.8 ± 0.1	29.5
YZ130	5-SO <sub>3</sub> H- naphthalen-2-yl	NA	>1000
YZ131	4-SO <sub>3</sub> H- naphthalen-1-yl	NA	>1000
YZ132	4-SO <sub>3</sub> H- Ph	NA	NA
YZ133	6-Br-naphthalen-2-yl	NA	NA

YZ134	(N-ethyl)1,8-Naphthalimide-4-yl	NA	NA
YZ135	Coumarin-6-yl	9.3 ± 1.0	>1000
SKF96265		25.7 ± 1.0	NA
17-AAG		5.90	59.65

**Table S4.** Primers used in RT-PCR (COX2, MMP-7/9) and caCnA plasmid construction.  
(*Related to Figures 1 and 5*)

Genes	Primers
COX-2	5'-CAA AAG CTG GGA AGC CTT CTC TAA-3' (Forward)
	5'-GCC CAG CCC GTT GGT GAA AG-3' (Reverse)
MMP-7	5'-AAA CTC CCG CGT CAT AGA AAT-3' (Forward)
	5'-TCC CTA GAC TGC TAC CAT CCG-3' (Reverse)
MMP-9	5'-CAA ACC CTG CGT ATT TCC-3' (Forward)
	5'-AGA GTA CTG CTT GCC CAG GA-3' (Reverse)
GAPDH	5'-GCA CCG TCA AGG CTG AGAAC-3' (Forward)
	5'-TGG TGA AGA CGC CAGTGG A-3' (Reverse)
N-terminal catalytic domain of calcineurin (CnA; residues 1-381)	5'-CGG GAATTCATGTCCGAGCCCAAGGCGATTGATCCCAAG-3' (Forward)
	5'-CGGCTCGAGCTATTCTTCTGACCCAGTTCATCGTC-3' (Reverse)